

# Persistence of Gamma-H2AX Foci in Bronchial Cells Correlates with Susceptibility to Radiation Associated Lung Cancer in Mice

Authors: Ochola, Donasian O., Sharif, Rabab, Bedford, Joel S., Keefe,

Thomas J., Kato, Takamitsu A., et al.

Source: Radiation Research, 191(1): 67-75

Published By: Radiation Research Society

URL: https://doi.org/10.1667/RR14979.1

BioOne Complete (complete.BioOne.org) is a full-text database of 200 subscribed and open-access titles in the biological, ecological, and environmental sciences published by nonprofit societies, associations, museums, institutions, and presses.

Your use of this PDF, the BioOne Complete website, and all posted and associated content indicates your acceptance of BioOne's Terms of Use, available at <a href="https://www.bioone.org/terms-of-use">www.bioone.org/terms-of-use</a>.

Usage of BioOne Complete content is strictly limited to personal, educational, and non - commercial use. Commercial inquiries or rights and permissions requests should be directed to the individual publisher as copyright holder.

BioOne sees sustainable scholarly publishing as an inherently collaborative enterprise connecting authors, nonprofit publishers, academic institutions, research libraries, and research funders in the common goal of maximizing access to critical research.

RADIATION RESEARCH **191**, 67–75 (2019) 0033-7587/19 \$15.00 ©2019 by Radiation Research Society. All rights of reproduction in any form reserved. DOI: 10.1667/RR14979.1

# Persistence of Gamma-H2AX Foci in Bronchial Cells Correlates with Susceptibility to Radiation Associated Lung Cancer in Mice

Donasian O. Ochola, Rabab Sharif, Joel S. Bedford, Thomas J. Keefe, Takamitsu A. Kato, Christina M. Fallgren, Peter Demant, Sylvain V. Costes and Michael M. Weila, 1

<sup>a</sup> Department of Environmental and Radiological Health Sciences, Colorado State University, Fort Collins, Colorado; <sup>b</sup> Department of Molecular and Cellular Biology, Roswell Park Cancer Institute, Buffalo, New York; and <sup>c</sup> Biosciences Division, NASA Ames Research Center, Mountain View, California

Ochola, D. O., Sharif, R., Bedford, J. S., Keefe, T. J., Kato, T. A., Fallgren C. M., Demant, P., Costes, S. V. and Weil, M. M. Persistence of Gamma-H2AX Foci in Bronchial Cells Correlates with Susceptibility to Radiation Associated Lung Cancer in Mice. *Radiat. Res.* 191, 67–75 (2019).

The risk of developing radiation-induced lung cancer differs between different strains of mice, but the underlying cause of the strain differences is unknown. Strains of mice also differ in how quickly they repair radiation-induced DNA double-strand breaks (DSBs). We assayed mouse strains from the CcS/Dem recombinant congenic strain set for their efficacy in repairing DNA DSBs during protracted irradiation. We measured unrepaired  $\gamma$ -H2AX radiation-induced foci (RIF), which persisted after chronic 24-h gamma irradiation, as a surrogate marker for repair efficiency in bronchial epithelial cells for 17 of the CcS/Dem strains and the BALB/c founder strain. We observed a very strong correlation ( $R^2 = 79.18\%$ , P < 0.001) between the level of unrepaired RIF and radiogenic lung cancer incidence measured in the same strains. Interestingly, spontaneous levels of foci in nonirradiated mice also showed good correlation with lung cancer incidence when incidence data from male and female mice were combined. These results suggest that genetic differences in DNA repair capacity largely account for differing susceptibilities to radiationinduced lung cancer among CcS/Dem mouse strains, and that high levels of spontaneous DNA damage are also a relatively good marker of cancer predisposition. In a smaller pilot study, we found that the repair capacity measured in peripheral blood leucocytes also correlated well with radiogenic lung cancer susceptibility, raising the possibility that the assay could be used to detect radiogenic lung cancer susceptibility in humans. © 2019 by Radiation Research Society

*Editor's note.* The online version of this article (DOI: 10.1667/RR14979.1) contains supplementary information that is available to all authorized users.

<sup>1</sup> Address for correspondence: 1618 Campus Delivery, Fort Collins, CO 80523; email: michael.weil@colostate.edu.

# INTRODUCTION

Radiation exposure carries with it an increased risk for lung cancer. This increased risk has been observed in atomic bomb survivors (1) and in cohorts with medical [(2–4); reviewed in (5)], occupational and environmental radiation exposures (6). Radiation-induced lung cancer remains a concern for radiotherapy patients, and radiogenic lung cancer is a risk factor limiting flight times for spaceflight crew members (7). There is some evidence to suggest a genetic susceptibility to radiogenic lung cancer in humans (8), but the relative contributions of the pathways through which naturally occurring genomic sequence variants are manifested (e.g., DNA repair, apoptosis, EGFR signaling) are unknown.

Inbred mouse strains differ in their susceptibilities to radiogenic cancers, including lung cancer (9), and these strain differences in susceptibility are likely due to genetic differences between strains. The CcS/Dem recombinant congenic strain set consists of 20 inbred strains (CcS1 through CcS20) derived from the BALB/cHeA and STS/A founder strains (10, 11). Each CcS/Dem strain is genetically distinct and has approximately 87.5% of its genome derived from the BALB/c founder and the remainder from STS/A. The strains have been phenotyped for their incidences of radiation-induced lung cancers and hematopoietic malignancies, and vary considerably in their susceptibilities to both (11).

Ionizing radiation induces DNA double-strand breaks (DSBs), and the misrepair of these lesions can contribute to carcinogenesis. Individuals differ in their capacity to efficiently repair DNA DSBs, and there are also differences in repair efficiencies among mouse strains. It has been 20 years since the discovery that the histone variant H2AX is specifically modified only at DSB sites (I2), giving rise to immunofluorescent techniques and a quantitative surrogate marker for radiation-induced DSBs in eukaryotic cells (I3). Capitalizing on this discovery, we previously introduced the LDR  $\gamma$ -H2AX assay, which is a sensitive assay reflecting the repair efficacy of radiation-induced DNA DSBs based

on evaluating the persistence of γ-H2AX foci in cells irradiated at low dose rate. The assay detects mild DNA repair deficiency in human ATM heterozygotes and Atm<sup>+/-</sup> mice (14, 15), as well as repair differences among clinically normal individuals (16). Here, we phenotyped the CcS/Dem strains for their DNA DSB break repair efficiencies using the same LDR y-H2AX assay and compared the results to those obtained for their susceptibilities to radiogenic lung cancer in a previously published study (11). We found a strong correlation between the strain differences in susceptibility to radiation-associated lung cancer and the persistence of  $\gamma$ -H2AX foci in irradiated bronchial epithelial cells. The correlation extends to the baseline damage in nonirradiated bronchial epithelial cells for all strains, as well as in leucocytes from irradiated animals from a smaller cohort of strains. Within the CcS/Dem strain set, genetically determined differences in DNA DSB repair account for most of the differences between strains in radiogenic lung cancer incidence. This finding suggests that assays to predict individual susceptibility to radiation-induced lung cancers can be developed around the usage of both baseline levels of DNA damage and persistence of damage in irradiated cells.

## MATERIALS AND METHODS

Mice

Female CcS/Dem, STS/A and BALB/cHeA mice were assayed at 11 to 15 weeks of age. All animal work complied with American Association for Laboratory Animal Science policies and was approved by the Colorado State University Institutional Animal Care and Use Committee under protocol no. 09-1582A.

# Irradiation

Mice were irradiated with  $^{137}\text{Cs}$   $\gamma$  rays at a dose rate of 10 cGy/h for 24 h to a cumulative dose of 2.4 Gy. During irradiation the mice were housed in ventilated  $5\times5\times8$  cm polystyrene boxes with a cube of Nutra-Gel (Bio-Serv®, Flemington, NJ) for food and hydration. Four mice of each strain were assayed, with the exception of CcS13 for which only three mice were available. Sham-irradiated mice that served as controls were treated under similar conditions, but without exposure to the  $^{137}\text{Cs}$  source.

# Tissue Collection

Mice were euthanized immediately after irradiation and their lungs were perfused *in situ*. Fixed lung tissue was paraffin embedded and sectioned for  $\gamma$ -H2AX foci detection by immunofluorescence. For foci detection in peripheral blood mononuclear cells, heparinized blood was collected by cardiac puncture, and erythrocytes lysed with distilled water. The leucocytes were then deposited onto slides, and fixed (detailed methods are provided in Supplementary Information; http://dx.doi.org/10.1667/RR14979.1.S1).

# Immunofluorescence Staining and Quantitation of Foci

Paraffin-embedded samples were de-waxed and rehydrated by the standard method followed by antigen retrieval with sodium citrate and microwave (17). Leucocyte samples were treated with sodium borohydride solution to reduce autofluorescence background signals (18). Slides were stained by anti-γ-H2AX antibody (Millipore,

Burlington, MA) and Alexa Fluor® 594 conjugated secondary antibody, and counterstained with DAPI.

Extended focus images were obtained using a Nikon E600 fluorescence motorized microscope with CoolSNAP HQ camera controlled by OptiScan  $^{\text{TM}}$  stage system (Prior Photometrics, Tuscon, AZ) and MetaMorph® Software (Molecular Devices, Sunnyvale, CA). Visual counting was performed to quantify the foci number per cell. Cells with diffuse  $\gamma\text{-H2AX}$  staining suggestive of apoptosis were not counted.

#### Data Analysis

Summary statistics, which included the number of mice (n) per strain and the mean and standard deviation (SD) of the foci counts weighted by the number of cells counted per mouse by observer 1 or observer 2 (102.2  $\pm$  1.6 and 80.8  $\pm$  39.4, respectively), were calculated using Minitab® statistical software, release 17 (State College, PA). The Pearson correlation coefficient was calculated for the relationship between DNA repair efficiency (as measured by the mean number of foci per nucleus) and the incidence of radiation-associated lung tumors using GraphPad Prism software (San Diego, CA).

## RESULTS

It was previously shown elsewhere that CcS/Dem strains and one of their founder strains, BALB/cHeA, differ in their susceptibilities to radiogenic lung cancer, lymphomas and leukemias (11). The other founder strain, STS/A, was not tested. In that study, mice of both sexes were whole-body irradiated with four 1.5 Gy weekly fractions and monitored until they became moribund or reached 450 days of age. The incidences of lung cancer in the strains, originally reported in Szymanska *et al.* (11), are provided in Table 1.

We considered the possibility that strain differences in the efficacy of DNA DSB repair might account for the strain differences in radiogenic lung cancer susceptibility. To quantify DNA DSB repair efficacy, we used the low-doserate γ-H2AX assay, which we have described elsewhere (14–16). This assay measures differences in the DNA DSB repair capacities of cells by irradiating them at low dose rate over 24 h, a condition which results in the greater accumulation of DSBs in those cells that have less efficient DNA DSB repair. The DNA DSBs remaining in the cells immediately after the 24 h exposure are quantified as γ-H2AX foci. Presumably, greater numbers of foci persisting at the end of the protracted exposure indicate less efficient repair. Our previously work with this assay involved irradiation of cells in vitro. However, since the target cells for radiogenic lung cancer are thought to be bronchial epithelial cells, in this study we irradiated live mice from 17 of the CcS/Dem strains and the BALB/c and STS/A founder strains at low dose rate for 24 h, instead. Immediately after irradiation, the mice were euthanized, their lungs perfused with fixative to stop further DNA damage-related processing, and the γ-H2AX foci in their bronchial epithelial cells were detected by immunohistochemistry of paraffin-embedded sections.

The foci were not uniformly distributed among the cell types in the lung. More  $\gamma$ -H2AX foci formed in the

| TABLE 1                                  |             |
|--|-------------|
| Incidence of Lung Tumors in Irradiated M | <b>Iice</b> |

|        |        | No. of | No. of |           |        |        | No. of | No. of |           |
|--------|--------|--------|--------|-----------|--------|--------|--------|--------|-----------|
| Strain | Sex    | mice   | tumors | Incidence | Strain | Sex    | mice   | tumors | Incidence |
| BALB/c | Female | 42     | 15     | 36        | CcS-11 | Female | 42     | 9      | 21        |
|        | Male   | 32     | 14     | 44        |        | Male   | 40     | 14     | 35        |
|        | Both   | 74     | 29     | 39        |        | Both   | 82     | 23     | 28        |
| CcS-1  | Female | 43     | 14     | 33        | CcS-12 | Female | 45     | 15     | 33        |
|        | Male   | 37     | 12     | 32        |        | Male   | 42     | 6      | 14        |
|        | Both   | 80     | 26     | 33        |        | Both   | 87     | 21     | 24        |
| CcS-2  | Female | 41     | 9      | 22        | CcS-13 | Female | 42     | 12     | 29        |
|        | Male   | 40     | 17     | 43        |        | Male   | 45     | 19     | 42        |
|        | Both   | 81     | 26     | 32        |        | Both   | 87     | 31     | 36        |
| CcS-3  | Female | 42     | 14     | 33        | CcS-14 | Female | 42     | 6      | 14        |
|        | Male   | 40     | 17     | 43        |        | Male   | 42     | 4      | 10        |
|        | Both   | 82     | 31     | 38        |        | Both   | 84     | 10     | 12        |
| CcS-4  | Female | 40     | 19     | 48        | CcS-15 | Female | 37     | 5      | 14        |
|        | Male   | 35     | 13     | 37        |        | Male   | 42     | 12     | 29        |
|        | Both   | 75     | 32     | 43        |        | Both   | 79     | 17     | 22        |
| CcS-5  | Female | 47     | 11     | 23        | CcS-16 | Female | 30     | 8      | 27        |
|        | Male   | 40     | 10     | 25        |        | Male   | 35     | 6      | 17        |
|        | Both   | 87     | 21     | 24        |        | Both   | 65     | 14     | 22        |
| CcS-6  | Female | 23     | 2      | 9         | CcS-17 | Female | 28     | 8      | 29        |
|        | Male   | 17     | 0      |           |        | Male   | 32     | 10     | 31        |
|        | Both   | 40     | 2      | 5         |        | Both   | 60     | 18     | 30        |
| CcS-7  | Female | 32     | 6      | 19        | CcS-18 | Female | 42     | 7      | 17        |
|        | Male   | 24     | 1      | 4         |        | Male   | 42     | 6      | 14        |
|        | Both   | 56     | 7      | 13        |        | Both   | 84     | 13     | 15        |
| CcS-8  | Female | 44     | 4      | 9         | CcS-19 | Female | 40     | 12     | 30        |
|        | Male   | 42     | 9      | 21        |        | Male   | 40     | 14     | 35        |
|        | Both   | 86     | 13     | 15        |        | Both   | 80     | 26     | 33        |
| CcS-9  | Female | 45     | 13     | 29        | CcS-20 | Female | 43     | 17     | 40        |
|        | Male   | 37     | 16     | 43        |        | Male   | 46     | 21     | 46        |
|        | Both   | 82     | 29     | 35        |        | Both   | 89     | 38     | 43        |
| CcS-10 | Female | 41     | 5      | 12        |        |        |        |        |           |
|        | Male   | 47     | 4      | 9         |        |        |        |        |           |
|        | Both   | 88     | 9      | 10        |        |        |        |        |           |

epithelial cells of the conducting airways (comprising the bronchi and bronchioles) than in the respiratory airways (the alveoli). Within the conducting airways more foci formed in basal calls than in apical cells of the epithelium (Fig. 1). As

previously noted by Rübe *et al.* (19), there were also fewer foci formed in the stromal cell nuclei in the parenchyma of the lung in irradiated mice. We counted foci in bronchial epithelial cells and found considerable differences between

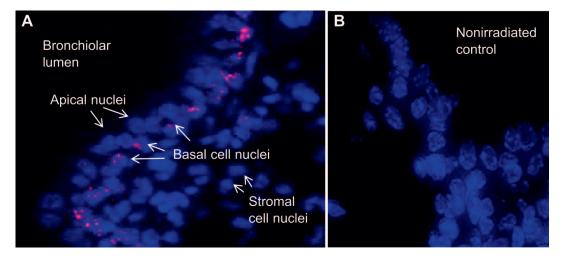


**FIG. 1.** Panel A: Section of irradiated lung showing many radiation-induced foci formed in the basal epithelial cells compared to the apical cells or stromal cells. Panel B: Similarly processed lung section from an unirradiated control mouse.

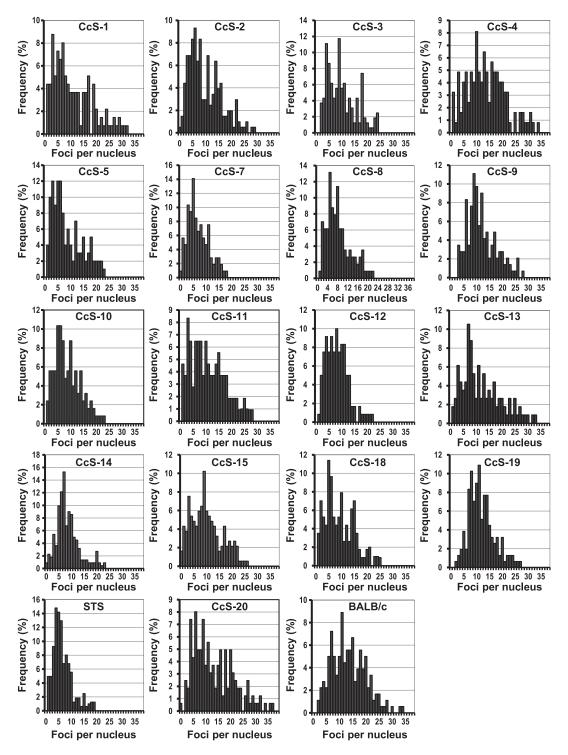


**FIG. 2.** Frequency histograms of the number of  $\gamma$ -H2AX foci per cell in lung basal epithelial cells in CcS/Dem and founder strains. The more efficient the strain in DSB repair, the more its histogram will be skewed to the left.

the strains (Fig. 2, Table 2). Since the bronchial epithelial cells are identified histologically by their positions within the tissue, our computer algorithms (20-22) could not be used here and we had to rely on human counts. As we have reviewed extensively in the past (23), manual foci counting can be affected by large inter-observer variability. To

account for this, foci were counted by two different individuals, both blinded to the lung cancer incidences in the different strains.

To determine if strains with less efficient repair were at greater risk for radiogenic lung cancer, we computed the Pearson's correlation between lung cancer incidence (11)

| TABLE 2   |
|---|
| Summary Statistics for the Average Number of Foci per Cell Based on Counts by |
| Two Independent Observers   |

|        | Observer 1 Average foci/cell |                                 |         |        | Observer 2 Average foci/cell |                                 | Cells   |
|--------|------------------------------|---------------------------------|---------|--------|------------------------------|---------------------------------|---------|
|        |                              |                                 | Cells   |        |                              |                                 |         |
| Strain | Mean                         | Standard deviation <sup>a</sup> | counted | Strain | Mean                         | Standard deviation <sup>a</sup> | counted |
| BALB/c | 19.77                        | 1.30                            | 400     | BALB/c | 17.10                        | 0.59                            | 396     |
| CcS1   | 17.83                        | 1.42                            | 412     | CcS1   | 17.63                        | 1.55                            | 744     |
| CcS2   | 18.08                        | 1.11                            | 432     | CcS2   | 17.20                        | 1.03                            | 564     |
| CcS3   | 18.30                        | 1.09                            | 412     | CcS3   | 14.30                        | 0.67                            | 360     |
| CcS4   | 23.13                        | 1.60                            | 400     | CcS4   | 21.51                        | 0.72                            | 372     |
| CcS5   | 12.55                        | 0.87                            | 404     | CcS5   | 14.18                        | 0.46                            | 258     |
| CcS7   | 11.17                        | 1.09                            | 408     | CcS7   | 11.51                        | 1.13                            | 246     |
| CcS8   | 11.05                        | 1.24                            | 412     | CcS8   | 12.45                        | 0.98                            | 240     |
| CcS9   | 19.28                        | 0.76                            | 408     | CcS9   | 11.32                        | 0.55                            | 240     |
| CcS10  | 8.70                         | 0.93                            | 408     | CcS10  | 9.94                         | 0.64                            | 252     |
| CcS11  | 16.52                        | 0.94                            | 408     | CcS11  | 15.47                        | 0.36                            | 240     |
| CcS12  | 13.67                        | 1.35                            | 408     | CcS12  | 11.42                        | 0.52                            | 282     |
| CcS13  | 20.13                        | 1.52                            | 306     | CcS13  | 16.10                        | 0.22                            | 216     |
| CcS14  | 8.15                         | 0.88                            | 408     | CcS14  | 9.60                         | 1.03                            | 240     |
| CcS15  | 14.47                        | 1.40                            | 408     | CcS15  | 14.03                        | 0.47                            | 240     |
| CcS18  | 9.95                         | 0.72                            | 408     | CcS18  | 10.10                        | 0.71                            | 240     |
| CcS19  | 17.07                        | 0.91                            | 408     | CcS19  | 14.80                        | 0.98                            | 240     |
| CcS20  | 22.90                        | 1.71                            | 408     | CcS20  | 18.94                        | 1.03                            | 240     |
| STS/A  | 6.72                         | 0.92                            | 404     | STS    | 6.61                         | 1.37                            | 234     |
| All    | 15.17                        | 4.99                            | 7662    | All    | 14.64                        | 3.73                            | 5,844   |

Note. Three mice were assayed for CcS13, four mice were assayed for all other strains.

and average number of foci in irradiated mice for each strain (except STS/A, for which incidence data are not available). Since the foci data were from female mice, they were compared first to lung cancer incidence in female mice. However, for some strains, relatively few female mice had been tested for radiation-induced lung cancer, so a comparison was also made to lung cancer incidence in both sexes combined. The caveat with this approach is that for a number of other radiogenic tumors for which larger datasets are available, there are sex differences in incidence. Strong correlations between foci levels measured in female mice and lung cancer incidence were found by both observers ( $R^2 = 60.6\%$ , P < 0.001 for the incidence in female mice and  $R^2 = 79.2\%$ , P < 0.001 for the incidence in both sexes) (Fig. 3). However, the foci counts of observer 1 were more closely correlated with incidence than those of observer 2 (observer 1,  $R^2 = 95.7\%$ , P < 0.001; observer 2,  $R^2 = 68.5\%$ , P < 0.001 for the correlations with incidence in both sexes). The inter-observer difference is likely due to the selection of cells in which to count foci.

DNA DSBs can occur spontaneously in the absence of radiation, which would lead to background  $\gamma$ -H2AX foci in our assay. To determine foci numbers in the bronchial epithelial cells of nonirradiated mice, we counted foci in four nonirradiated female BALB/c mice (observer 1 only). The average foci number per nucleus was low, at 3.25. To ensure that none of the CcS/Dem strains was an outlier with high levels of spontaneous foci, we surveyed one mouse from each strain and found a range between 1.5 and 2.8 foci per nucleus (Table 3). Although the data on background foci

levels were limited, coming from only a single mouse per strain (with the exception of BALB/c), and the differences among the strains were not large, we tested for a correlation between background foci and lung cancer incidence. Somewhat surprisingly, we found a significant correlation between background foci and lung cancer incidence in both sexes; the correlation between background foci and lung cancer incidence in female mice did not reach significance (Fig. 3).

To determine if strain differences in DNA DSB repair efficiencies in peripheral blood leukocytes correlated with repair efficiencies in bronchial epithelial cells or with radiogenic lung cancer susceptibility, we undertook a more limited experiment in which we irradiated additional BALB/ c and STS/A mice, and mice from four CcS/Dem strains that had high, low and intermediate repair efficiencies in their bronchial epithelial cells. The foci were counted by observer 1 and the results are shown in Table 4. Although the observer attempted to count foci only in lymphocytes based on nuclear morphology, monocytes could not be reliably excluded from the counts. However, monocytes comprise only approximately 5% of murine peripheral blood leucocytes compared to approximately 80% for lymphocytes. There was a strong correlation between foci counts in leukocytes and bronchial epithelial cells ( $R^2 = 91.57\%$ , P =0.003) (Fig. 4). The foci counts in leukocytes also correlated with lung cancer incidence in female mice ( $R^2 = 86.6\%$ , P =0.022), although the correlation with lung cancer incidence in both sexes did not reach significance ( $R^2 = 75.8\%$ , P =0.055) (Fig. 5). The results indicate that the repair capacity

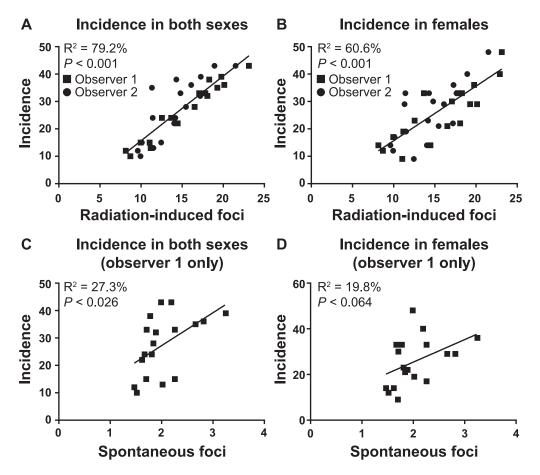


**FIG. 3.** Panels A and B: Correlation between repair efficiencies and radiogenic lung cancer incidences in both sexes and in female mice only, respectively, of the BALB/c and CcS/Dem strains. Repair efficiencies are expressed as foci counts per nucleus in bronchial epithelial cells quantified in the LDR  $\gamma$ -H2AX assay, with more foci indicating less efficient repair. To account for inter-observer variability, the foci counts for both observers (1 and 2) are plotted, and the correlation of foci to incidence is calculated using all of the data points. Panels C and D: Correlation between spontaneous  $\gamma$ -H2AX foci in nonirradiated mice (both sexes and females only, respectively) and radiogenic lung cancer incidences (observer 1 only).

in peripheral blood leucocytes is a good predictor of radiogenic lung cancer susceptibility in these strains.

# DISCUSSION

A major finding that emerged from this study is that most of the variance in susceptibility to radiogenic lung cancer in the CcS/Dem strains can be attributed to strain differences in DNA DSB repair efficiencies detectable by the LDR γ-H2AX assay. The R<sup>2</sup> for the combined foci counts of both observers in both sexes was 79%, suggesting 79% of the variance in lung cancer susceptibility is explained by differences in repair capacity. Since the laboratory mice that comprise the CcS/Dem strain set ultimately trace back to wild populations, an implication of this finding is that naturally occurring differences in DNA DSB repair efficiency that could result in interindividual differences in radiogenic lung cancer susceptibility exist within these populations. Might this also be the case for humans? We have reported differences in repair efficiencies in human fibroblasts from different normal donors detected using the

LDR  $\gamma$ -H2AX assay, with approximately 40% of those screened having less efficient repair. The magnitudes of the strain or interindividual differences are comparable between mice and humans [the mean foci count in fibroblasts from 15 normal human donors ranged from 4.5–11.3 per nucleus (*16*); for bronchial epithelial cells in the 17 CcS/Dem strains assayed the range was 8.2–23.1 foci per nucleus].

However, a couple of caveats need to be considered in extrapolating our findings in recombinant congenic mice to wider populations and to humans. The first is in extrapolating the magnitude of an effect determined in a strain set to a general population. There is limited genetic diversity in the CcS/Dem strains. There can be at most two alleles for each locus, since the set derives from two inbred founder strains. So, while differences in susceptibility between BALB/c and CcS/Dem strains can be largely or entirely explained by their differing repair capacities, there may be other collections of inbred strains that differ in susceptibility due to other causes. By extension to humans, differences in DNA DSB repair efficiencies in a general population may explain only part of the variance in lung

TABLE 3
Spontaneous Foci in Bronchial Epithelial Cells from
Nonirradiated Mice

|                     | 11   | omiradiated whice  |               |  |  |
|---------------------|------|--------------------|---------------|--|--|
|                     | A    | Average foci/cell  |               |  |  |
| Strain <sup>a</sup> | Mean | Standard deviation | Cells counted |  |  |
| BALB/c              | 3.25 | 0.09               | 408           |  |  |
| STS/A               | 1.40 | 0.03               | 312           |  |  |
| CcS1                | 2.26 | 0.29               | 312           |  |  |
| CcS2                | 1.89 | 0.11               | 306           |  |  |
| CcS3                | 1.78 | 0.10               | 306           |  |  |
| CcS4                | 1.99 | 0.17               | 306           |  |  |
| CcS5                | 1.81 | 0.13               | 306           |  |  |
| CcS7                | 2.02 | 0.43               | 306           |  |  |
| CcS8                | 1.70 | 0.08               | 306           |  |  |
| CcS9                | 2.66 | 0.11               | 306           |  |  |
| CcS10               | 1.52 | 0.08               | 306           |  |  |
| CcS11               | 1.84 | 0.07               | 306           |  |  |
| CcS12               | 1.67 | 0.08               | 306           |  |  |
| CcS13               | 2.82 | 0.15               | 306           |  |  |
| CcS14               | 1.47 | 0.07               | 306           |  |  |
| CcS15               | 1.62 | 0.15               | 306           |  |  |
| CcS18               | 2.26 | 0.32               | 306           |  |  |
| CcS19               | 1.71 | 0.11               | 306           |  |  |
| CcS20               | 2.19 | 0.06               | 306           |  |  |
| All                 | 2.01 | 0.52               | 5,928         |  |  |

<sup>&</sup>quot; Four mice were assayed for BALB/c. For all other strains, three separate tissue sections from an individual mouse were assayed.

cancer susceptibility. The second caveat is that, clearly, there are likely to be differences between the pathogenesis of radiation-induced lung cancers in mice and humans, so further study will be necessary to link repair proficiency with radiogenic lung cancer in humans.

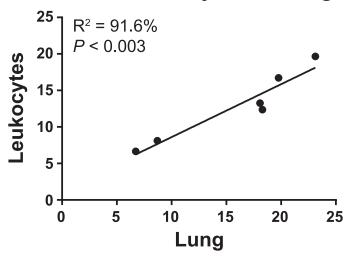
There is a significant correlation between spontaneous  $\gamma$ -H2AX foci levels in the bronchial epithelial cells in nonirradiated mice and radiogenic lung cancer incidence in both sexes (the correlation with incidence data from female mice only is not quite significant, probably because it derives from fewer mice). This finding supports the concept that baseline damage levels in an individual are the net balance between spontaneous damage being generated in the tissue and the efficiency of the repair machinery constantly clearing the damage (24). In CcS/Dem recombinant congenic mice, strain differences in spontaneous DNA DSB repair efficiency are amplified by radiation exposure.

TABLE 4
Foci in Peripheral Blood Leucocytes

|                     |       | 1                  | <u> </u>      |
|---------------------|-------|--------------------|---------------|
| Strain <sup>a</sup> | Mean  | Standard deviation | Cells counted |
| BALB/c              | 16.72 | 0.57               | 228           |
| STS/A               | 6.70  | 0.16               | 264           |
| CcS2                | 13.31 | 0.72               | 238           |
| CcS3                | 12.35 | 0.76               | 255           |
| CcS4                | 19.68 | 0.73               | 228           |
| CcS10               | 8.11  | 0.26               | 242           |
| All                 | 12.61 | 4.54               | 1,455         |

<sup>&</sup>lt;sup>a</sup> Four mice were assayed for each strain.

# Foci in leukocytes and lung



**FIG. 4.** Correlation between repair efficiencies in peripheral blood leucocytes and bronchial epithelial cells in BALB/c, STS/A and CcS/Dem strains, CcS2, CcS3, CcS4 and CcS10.

The finding that strain differences in repair efficiency measured in peripheral blood leucocytes mirror those in bronchial epithelial cells and consequently correlate with radiogenic lung cancer is not surprising. We demonstrated that the LDR y-H2AX assay distinguished individuals with one defective copy of ATM from individuals with two defective copies or two normal copies, regardless of whether the assay employed fibroblasts or lymphoblasts (15). In mice, Rübe et al. (25) followed the kinetics of DNA DSB repair in two traditional laboratory mouse strains (BALB/c and C57BL/6), a strain homozygous for a knockout allele of Atm, and a SCID strain with a spontaneous mutation in the gene encoding the catalytic subunit of DNA-dependent protein kinase (Prkdc). The latter two strains have profound defects in DNA DSB repair. They observed that the rank order of repair efficiencies among the four strains of mice was the same regardless of the tissues assayed (lung, brain, heart or intestine irradiated in vivo, and peripheral blood lymphocytes irradiated ex vivo). Unlike bronchial epithelial cells, peripheral blood cells are readily accessible; so, it should be possible to test for a correlation between repair efficiency of peripheral blood lymphocytes irradiated ex vivo and radiogenic cancer susceptibility in humans if a suitable cohort could be identified.

How might slower repair of radiation-induced DSBs increase cancer risk? Consider the mechanism favored to explain the linear-quadratic dose-response relationship observed for chromosomal aberrations (26), which are known to be a direct cause of certain leukemias and solid cancers. The relationship describes how at lower radiation doses the numbers of chromosomal aberrations per nucleus are proportional to dose, but at higher doses the numbers of chromosomal aberrations are proportional to the square of

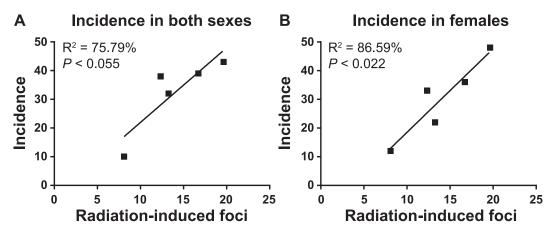


FIG. 5. Correlation between repair efficiencies in peripheral blood leucocytes and radiogenic lung cancer incidences in BALB/c and CcS/Dem strains, CcS2, CcS3, CcS4 and CcS10.

the dose; that is, they increase at a greater rate. According to most evidence, the large majority of the aberrations are exchanges that occur between radiogenic breaks on different chromosomes (or regions within a single chromosome). These break pairs need to be contemporaneous (close in both time and space) for the misrejoining to occur. At low doses where only one or a few breaks are present per nucleus, there is less opportunity for misrejoining events leading to chromosomal aberrations because there are fewer noncontiguous ends available for misrejoining. Restitution (eurepair), whereby the broken ends on either side of a single break site rejoin to reconstitute continuity of the damaged chromosome, is favored. At higher doses, there are more noncontiguous broken ends available for misrejoining and, consequently, more chromosomal aberrations.

The same logic applies to inefficient repair. In an irradiated cell, the actual number of DSBs at a given time depends not only on the dose received, but also on how quickly the cell repairs the breaks. If the repair is efficient, fewer DSBs will be present concurrently, the opportunity for misrejoining will be lower and there will be fewer chromosomal aberrations than if repair is inefficient. Cells with inefficient DNA DSB repair will have more DSBs per nucleus present over a longer time than cells with efficient repair. Thus, inefficient repair leads to more misrepair and, consequently, greater mutational load and cancer risk.

## SUPPLEMENTARY INFORMATION

Detailed methods of tissue collection, immunofluorescent staining and foci quantification.

# ACKNOWLEDGMENTS

This work was supported by the U.S. Department of Energy (DOE grant no. DE-FG03-01ER63365 to JSB) and the National Aeronautics and Space Administration (NASA grant no. NNX15AK13G to MMW). We

thank Dr. Michael Cornforth, University of Texas Medical Branch, for helpful discussions.

Received: November 2, 2017; accepted: October 4, 2018; published online: November 6, 2018

#### REFERENCES

- Preston DL, Ron E, Tokuoka S, Funamoto S, Nishi N, Soda M, et al. Solid cancer incidence in atomic bomb survivors: 1958–1998. Radiat Res 2007; 168:1–64.
- Gilbert ES, Stovall M, Gospodarowicz M, Van Leeuwen FE, Andersson M, Glimelius B, et al. Lung cancer after treatment for Hodgkin's disease: focus on radiation effects. Radiat Res 2003; 159:161–73.
- Travis LB, Gospodarowicz M, Curtis RE, Clarke EA, Andersson M, Glimelius B, et al. Lung cancer following chemotherapy and radiotherapy for Hodgkin's disease. J Natl Cancer Inst 2002; 94:182–92.
- van Leeuwen FE, Klokman WJ, Stovall M, Hagenbeek A, van den Belt-Dusebout AW, Noyon R, et al. Roles of radiotherapy and smoking in lung cancer following Hodgkin's disease. J Natl Cancer Inst 1995; 87:1530–7.
- Second primary cancers and cardiovascular disease after radiation therapy. NCRP Report No. 170. Bethesda: National Council on Radiation Protection and Measurements; 2011.
- BIER VI Health Effects of Exposure to Radon. Washington, DC: National Research Council; 1999.
- Cucinotta FA, Kim MY, Chappell LJ. Space radiation cancer risk projections and uncertainties - 2012. Report No. NASA/TP-2013-217375. Washington, DC: National Aeronautics and Space Administration; 2013.
- Yoshida K, Nakachi K, Imai K, Cologne JB, Niwa Y, Kusunoki Y, et al. Lung cancer susceptibility among atomic bomb survivors in relation to CA repeat number polymorphism of epidermal growth factor receptor gene and radiation dose. Carcinogenesis 2009; 30:2037–41.
- Storer JB, Mitchell TJ, Fry RJ. Extrapolation of the relative risk of radiogenic neoplasms across mouse strains and to man. Radiat Res 1988; 114:331–53.
- Demant P, Hart AA. Recombinant congenic strains—a new tool for analyzing genetic traits determined by more than one gene. Immunogenetics 1986; 24:416–22.
- Szymanska H, Sitarz M, Krysiak E, Piskorowska J, Czarnomska A, Skurzak H, et al. Genetics of susceptibility to radiation-induced

- lymphomas, leukemias and lung tumors studied in recombinant congenic strains. Int J Cancer 1999; 83:674–78.
- Rogakou EP, Pilch DR, Orr AH, Ivanova VS, Bonner WM. DNA double-stranded breaks induce histone H2AX phosphorylation on serine 139. J Biol Chem 1998; 273:5858–68.
- Nelms BE, Maser RS, MacKay JF, Lagally MG, Petrini JH, In situ visualization of DNA double-strand break repair in human fibroblasts. Science 1998; 280:590–2.
- 14. Kato TA, Nagasawa H, Weil MM, Genik PC, Little JB, Bedford JS. Gamma-H2AX foci after low dose-rate irradiation reveal mouse Atm haploinsufficiency. Radiat Res 2006, 166:47–54.
- 15. Kato TA, Nagasawa H, Weil MM, Little JB, Bedford JS, Levels of gamma-H2AX Foci after low-dose-rate irradiation reveal a DNA DSB rejoining defect in cells from human ATM heterozygotes in two at families and in another apparently normal individual. Radiat Res 2006; 166:443–53.
- 16. Kato TA, Wilson PF, Nagasawa H, Fitzek MM, Weil MM, Little JB, et al. A defect in DNA double strand break processing in cells from unaffected parents of retinoblastoma patients and other apparently normal humans. DNA Repair (Amst) 2007; 6:818–29.
- 17. Shi SR, Chaiwun B, Young L, Cote RJ, Taylor CR. Antigen retrieval technique utilizing citrate buffer or urea solution for immunohistochemical demonstration of androgen receptor in formalin-fixed paraffin sections. J Histochem Cytochem 1993; 41:1599–604.
- Clancy B, Cauller LJ. Reduction of background autofluorescence in brain sections following immersion in sodium borohydride. J Neurosci Methods 1998; 83:97–102.
- 19. Rube CE, Grudzenski S, Kühne M, Dong X, Rief N, Lobrich M, et

- al. DNA double-strand break repair of blood lymphocytes and normal tissues analysed in a preclinical mouse model: implications for radiosensitivity testing. Clin Cancer Res 2008; 14:6546–55.
- Costes SV, Boissiere A, Ravani S, Romano R, Parvin B, Barcellos-Hoff MH. Imaging features that discriminate between foci induced by high- and low-LET radiation in human fibroblasts. Radiat Res 2006; 165:505–15.
- 21. Georgescu W, Osseiran A, Rojec M, Liu Y, Bombrun M, Tang J, et al. Characterizing the DNA damage response by cell tracking algorithms and cell features classification using high-content time-lapse analysis. PLoS One 2015; 10:e0129438.
- Neumaier T, Swenson J, Pham C, Polyzos A, Lo AT, Yang P, et al. Evidence for formation of DNA repair centers and doseresponse nonlinearity in human cells. Proc Natl Acad Sci U S A 2012; 109:443–8.
- Costes SV, Chiolo I, Pluth JM, Barcellos-Hoff MH, Jakob B. Spatiotemporal characterization of ionizing radiation induced DNA damage foci and their relation to chromatin organization. Mutat Res 2010; 704:78–87.
- 24. Rube CE, Fricke A, Widmann TA, Furst T, Madry H, Pfreundschuh M, et al. Accumulation of DNA damage in hematopoietic stem and progenitor cells during human aging. PLoS One 2011; 6:e17487.
- Rube CE, Dong X, Kuhne M, Fricke A, Kaestner L, Lipp P, et al. DNA double-strand break rejoining in complex normal tissues. Int J Radiat Oncol Biol Phys 2008; 72:1180–87.
- Lea DE, Catcheside DG. The mechanism of the induction by radiation of chromosome aberrations in Tradescantia. J Genet 1942; 44:216–45.